

Decoration of electrospun polyacrylonitrile nanofibers with ZnO nanoparticles and their application for removal of Pb ions from waste water

Nesa Rouhipour Mikal¹ · Sodeh Sadjadi² · Mehdi Rajabi-Hamane¹ · Seyed Javad Ahmadi² · Effat Iravani²

Received: 8 September 2015 / Accepted: 20 November 2015 / Published online: 30 November 2015
© Iranian Chemical Society 2015

Abstract The adsorption behavior of lead (II) from aqueous solutions utilizing ZnO/polyacrylonitrile (PAN) nanofibers was studied. ZnO/PAN nanofibers were prepared by electrospinning method. The changes of the parameters of adsorbent amount, pH, contact time, and temperature were tested in the adsorption experiments. The adsorption was well described by the Langmuir adsorption isotherm model. The thermodynamic parameters indicate that the adsorption process is exothermic. The dynamic behavior of the lead (II) ions adsorption by PAN/ZnO nanofibers was well described by the pseudo-second-order kinetic model. The adsorbent can be regenerated by suitable desorption processes for multiple uses without significant loss of its adsorption capacity.

Keywords Adsorption · Polyacrylonitrile · ZnO nanoparticles · Lead (II) ions · Nanofibers

Introduction

The presence of heavy metals in the environment is one of the major concerns because of their toxicity and threat to human life [1–3]. Many of these metals are required by humans in trace amounts, but in larger, persistent dosages, these heavy metals become toxic when they are not metabolized by the body and accumulate in the soft tissues [4]. Lead toxicity may cause adverse health effects such as anemia, encephalopathy, hepatitis, and nephritic syndrome [5].

Nanofibers are able to form a highly porous mesh and their large surface-to-volume ratio improves performance for many applications such as scaffolds in tissue engineering [6], drug delivery systems [7], nanofibrous membranes for fine filtration [8], and protective clothing [9]. The utilization of nanofibers is an attractive alternative to traditional separation methods due to their interesting characteristics such as high porosity, large surface area per unit mass, high gas permeability, and small interfibrous pore size [6] which lead to high adsorption rate and capacity as compared to other types of materials such as resins [10], foams [11], and conventional fibers [12].

Presently, the application of nanoparticle has emerged as a fascinating area of interest for removal of metallic pollutants from industrial effluents [13–17].

Over recent years, the incorporation of nanoparticles in the polymer nanofibres has received a tremendous amount of interest in the preparation of more effective nano-adsorbents system, implying a synergistic effect between the nanoparticles and nanofibres [18].

The ZnO nanoparticles with some features including high absorption of ultraviolet radiation and long life span [19] are widely used as catalyst [20], gas sensor [21], active filler in rubber and plastic, UV absorbent in cosmetics, and antivirus in coatings [22]. ZnO nanoparticles can be

✉ Sodeh Sadjadi
sadjadi.s.s@gmail.com
Nesa Rouhipour Mikal
n.rouhipour@ut.ac.ir
Mehdi Rajabi-Hamane
rajabi@ut.ac.ir
Seyed Javad Ahmadi
sjahmadi@yahoo.com
Effat Iravani
iravanieffat@yahoo.de

¹ School of Chemical Engineering, College of Engineering, University of Tehran, Tehran, Iran

² Nuclear Science and Technology Research Institute, End of North Karegar Ave., Po. Box: 14399-51113, Tehran, Iran

synthesized by various methods such as the sol–gel process, homogeneous deposition, mechanical synthesis, organometallic synthesis, sonochemistry, and thermal evaporation [23].

The sonochemistry method has been proven as a useful technique to obtain new materials with interesting properties which is based on the acoustic cavities resulting from the continuous formation, growth, and collapse of bubbles in a liquid. This method does not require high temperatures and surfactant [24].

In this study, the modified polyacrylonitrile (PAN) nanofibers with zinc oxide (ZnO) nanoparticles were synthesized. The prepared material was then used as adsorbent in the removal of lead ions in aqueous solution. The adsorption behavior of lead ions on this adsorbent has been studied and discussed.

Methods

Apparatus

Crystal structure of the prepared ZnO nanoparticles was analyzed using Cu K α radiation (Philips PW 1800, USA). Size and morphology of the obtained nanoparticles and nanofibers were observed by scanning electron microscopy (SEM, LEO1455VP, Germany). Thermal stability of the nanofibers was studied by thermogravimetric analysis (TG-DTA, STA 1500, UK) under air atmosphere at the heating rate of 283 K/min. IR spectra were recorded with a Bruker Vector 22 spectrometer (Germany) using KBr disks. Quantitative determinations of inorganic ions were carried out using an inductively coupled plasma atomic emission spectroscopy (ICP-AES, Optima 7300 DV, USA). The ultrasound apparatus was a cleaning bath Wiseclear 770 W (Seoul, Korea). The operating frequency was 40 kHz and the output power was 200 W.

Materials

All chemicals were of the highest purity available and used as received without further purification. PAN ($M_w = 150,000$), zinc acetate, tetra methyl ammonium hydroxide (TMAH), oleic acid (OLEA, 99 %), and toluene were purchased from Sigma (St. Louis, MO, USA). Dimethylformamide (DMF), ethanol, potassium chloride, and lead (II) nitrate were purchased from Merck (Darmstadt, Germany).

Synthesis of ZnO nanoparticles

To prepare ZnO nanoparticles, 250 ml of the solution (0.1 M) of $Zn(CH_3COO)_2$ in EtOH was posited in an

ultrasonic bath, then into this solution, 100 ml of TMAH solution (0.1 M) was added dropwise. After the end of TMAH addition, the solution was remained in the bath for 30 min at 313 K. The obtained precipitates were filtered by centrifuge, subsequently washed with EtOH and then dried. To form ZnO powders, the obtained precipitates were heated at 673 K in a furnace for 4 h.

In order to prepare ZnO nanoparticles that are dispersible in organic solvents and to reduce the aggregation among ZnO nanoparticles, an effective surface modification method was proposed by grafting oleic acid onto the ZnO particles. 1.5 ml of oleic acid was added to 50 ml *o*-xylene and then 1 g of nanoparticle powder was added to the solution. The obtained solution was refluxed for an hour at 323 K. Then the solution was centrifuged and the precipitate washed three times with toluene and dried at 343 K for 1 h. The OLEA-coated ZnO nanoparticles were then easily redispersed in dimethylformamide (DMF).

Synthesis of nanofiber containing ZnO nanoparticles

Fibers of PAN/ZnO were obtained by electrospinning. The PAN/DMF solution was prepared by dissolving 1 g PAN in 10 ml DMF, and then 0.01 or 0.03 g ZnO nanoparticles were added to this solution and dispersed using an ultrasonic apparatus for 2 h.

A homemade electrospinning setup consisted of a spinneret (metal needle), high-voltage supplier (DW-P503-4AC, Iran), ground collector and a syringe pump (JMS SP-510, Japan) was applied to fabricate PAN/ZnO fibers. The high-voltage supplier was used to connect metal needles and the grounded collector for forming electrostatic fields. The grounded collection roller covered with the aluminum foil was used to collect the nanofibers. The solution flow rate was controlled by a syringe pump.

The parameters of electrospinning were set as follows: voltage 18 kV, collecting distance between the syringe needle tip and the grounded collector 15 cm, and solution flow rate 2 ml/h.

Batch adsorption experiments

0.05 g of adsorbent was kept in 5 ml of 1.2×10^{-4} mol/l metal ion solutions at 298 ± 1 K for 5 h, with intermittent shaking to reach equilibrium. The solution was then filtered and metal ions were determined using ICP. Blank solutions were prepared without adsorbent, having the same concentration of metal ions. This solution was treated in the same way as above. The distribution coefficients (K_d) value was calculated by the following equation (Eq. 1, [25]):

$$K_d = \left[\frac{I - F}{F} \right] \frac{V}{M}, \quad (1)$$

where I and F are the initial and final concentration (mg/l) of metal ions in the solution phase, V is volume of initial solution in ml, and M is the dry mass of the adsorbent in g. Removal efficiency ($R\%$) of metal ions by the adsorbent is considered in percentage as Eq. (2), [26]:

$$\text{Removal efficiency } (R\%) = \frac{(I - F)}{I} \times 100 \quad (2)$$

The maximum capacity of adsorbents for K^+ in aqueous solutions was determined by batch equilibration of 0.03 g of nanofibers and 15 ml of 0.05 M of the KCl solution in a shaker water bath adjusted at 298 ± 1 K. After equilibration, the phases were separated and K^+ concentration was determined by flame atomic absorption spectroscopy analysis (FAAS). Capacity (mg/g) was calculated from Eq. (3), [27]:

$$\text{Capacity} = C_0 \times Z \times \frac{\% \text{Uptake}}{100} \times \frac{V}{m} \text{ mg/g}, \quad (3)$$

where

$$\% \text{Uptake} = (A_{\text{eq}}/A_0) \times 100$$

C_0 is the initial concentration of solution, (g/l), V is the solution volume (ml), m is the weight of the exchanger (g), and Z is the charge of the metal ion adsorbed. A_0 and A_{eq} are the initial amount of metal ion in the solution and the amount of metal ion adsorbed by adsorbent at equilibrium (g/l), respectively.

Results and discussion

Characterization

The XRD pattern of resulting ZnO nanoparticles is shown in Fig. 1. All the peaks in the diffraction diagram could be assigned to the hexagonal phase ZnO. The crystallographic phase is in good agreement with the standard data form JCPDS card no. 001-1136.

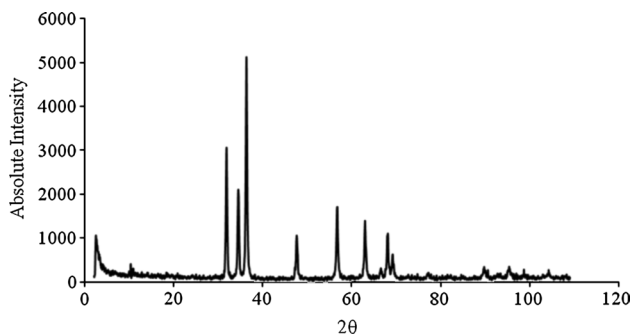


Fig. 1 XRD patterns of ZnO nanoparticles

The SEM image of the synthesized ZnO nanoparticles (Fig. 2) shows well-defined spherical shapes of the nanoparticles having a narrow size and shape distribution over the relevant size range 30–40 nm.

The PAN nanofibers were less than 20 nm in diameter, as can be seen in the SEM image (Fig. 3a). A piece of ZnO/PAN nanofibrous mat was stuck on a copper grid to observe the shape and distribution of nanoparticles in the PAN

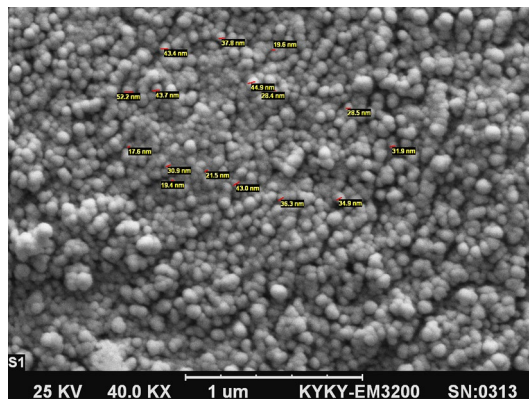


Fig. 2 SEM images of ZnO nanoparticles

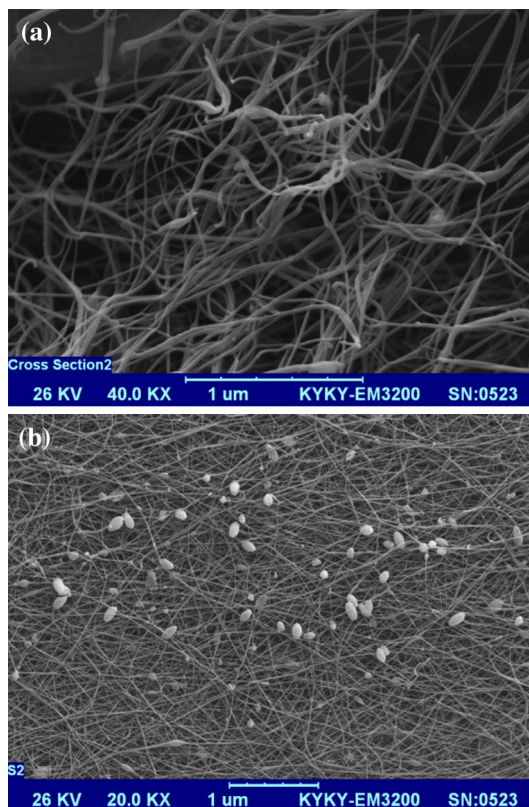


Fig. 3 SEM images a PAN nanofiber b PAN nanofiber amended by ZnO nanoparticles

nanofibers by SEM. Figure 3b shows the ZnO nanoparticles that existed on the surface of the nanofiber. However, a small part of the ZnO nanoparticles was distributed with some extent of aggregation.

Figure 4 shows the FT-IR analysis of the ZnO nanoparticles. Above 2000 cm^{-1} , C–H symmetric and asymmetric stretching vibrations in nearly 2851 and 2922 cm^{-1} are related to the $-\text{CH}_2-$ groups in the hydrocarbon part. Below 2000 cm^{-1} , COO^- symmetric and asymmetric stretching vibrations related to oleic acid carboxylate anions attached to the zinc are observed at 1629 and 1458 cm^{-1} , respectively. In 471 cm^{-1} , there is vibration specific to Zn–O inorganic bond.

Figure 5 is related to the FT-IR spectrometry analysis of PAN nanofibers amended by ZnO nanoparticles. By comparing the following diagram with Fig. 4, it can be observed that besides the bonds belonging to ZnO nanoparticles, there are also the vibrations of polyacrylonitrile, which include nitrile groups in 2248 cm^{-1} , carbonyl in 1728 cm^{-1} , and etheric bond (C–O) in 1070 cm^{-1} . C=O and C–O–C bands come from methylacrylate comonomer [28].

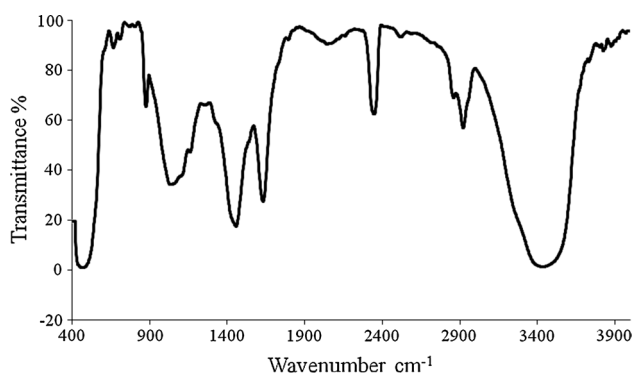


Fig. 4 FT-IR spectrum of as-prepared OLEA-capped ZnO nanoparticles

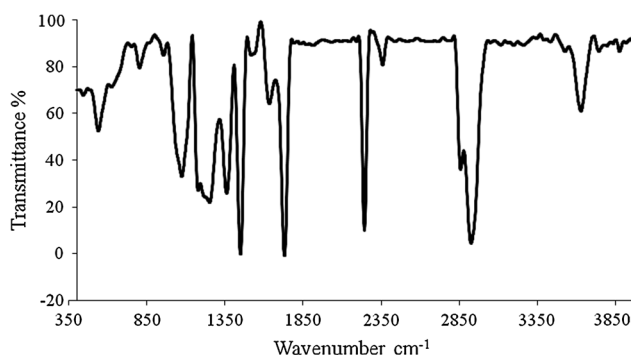


Fig. 5 FT-IR spectrum in the $400\text{--}4000\text{ cm}^{-1}$ region of PAN/ZnO nanofibers

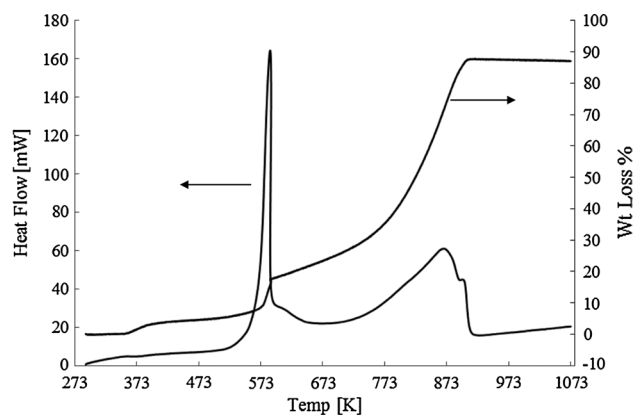


Fig. 6 Typical thermo gravimetric diagram for PAN/ZnO nanofibers

The thermal degradation of prepared nanofibers was performed with heating rate of 283 K min^{-1} in an air atmosphere (Fig. 6). The TGA curve shows a weight loss at two stages. The weight loss of the first stage, ranging between 573 and 623 K , could be attributed to the cyclization reaction of PAN and the evaporation of volatile materials (oleic acid) in the composition. The second stage of weight loss starts at about 883 K and continues up to 923 K is due to the degradation of polyacrylonitrile chains. This figure shows that ZnO nanoparticles are very stable in air and no decomposition takes place in the range of $293\text{--}1073\text{ K}$ [27].

The adsorption behavior of nanocomposite

Adsorption studies

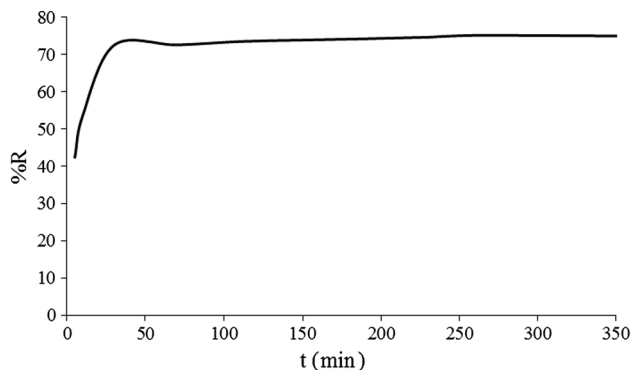
The prepared materials were then used as adsorbent in removal of lead ions in aqueous solution. To optimize the adsorption system, the effects of various parameters such as adsorbent type and dose, temperature, pH, concentration, and time on the adsorption of lead ions were studied.

Effect of adsorbent type The maximum adsorption capacity of three types of adsorbent (PAN fibers, PAN/ZnO nanofibers 1 and 3 %) was studied for K^+ . To investigate the effect of ZnO nanoparticles, we carried out the comparative experiments with PAN fibers loaded with different amounts of ZnO nanoparticles [1 g PAN, 0.01 g ZnO (1 %) and 1 g PAN, 0.03 g ZnO nanoparticles (3 %)]. The comparative results are summarized in Table 1. Loading a small amount of ZnO nanoparticles (1 %) into the PAN fibers results in the considerable enhancement of the adsorption capacity. An increase in ZnO nanoparticles loading results in increasing the adsorption capacity of nanofibers. Working with higher amounts of ZnO was not possible, because more than 3 % ZnO cannot be well dispersed in DMF. Thus PAN + 3 % ZnO nanocomposite was applied as an adsorbent of choice.

Table 1 The maximum adsorption capacity of synthesized adsorbents

Adsorbent	Capacity (mg/g)
PAN nanofibers	1.79
PAN + 1 % ZnO nanocomposite	4.38
PAN + 3 % ZnO nanocomposite	6.6

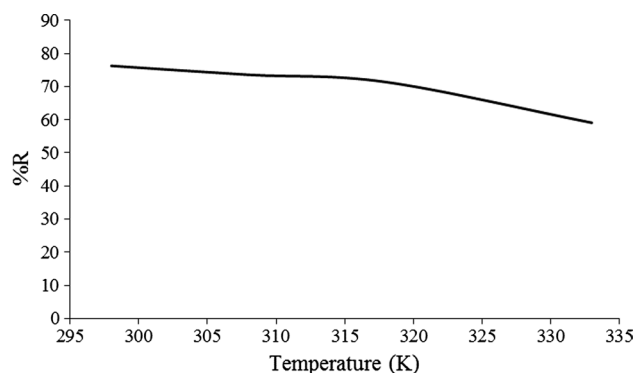
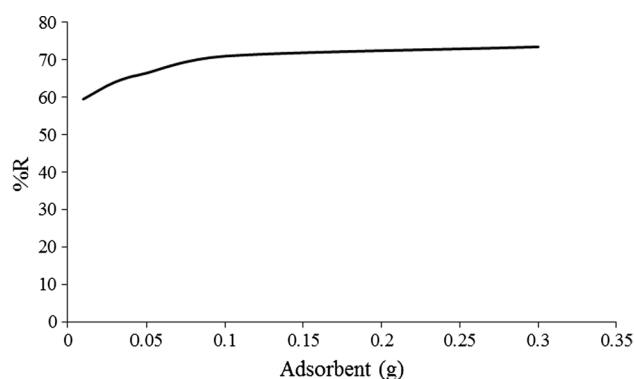
KCl = 0.05 mol/l, adsorbent weight = 0.03 g, 298 K, 24 h

**Fig. 7** The effect of contact time on adsorption of Pb^{2+} onto adsorbent [lead ions = 1.2×10^{-4} mol/l, pH 6, adsorbent (PAN + 3 % ZnO nanocomposite) weight = 0.03 g, 298 K]

The effect of contact time The influence of contact time on the adsorption of lead ions by PAN/ZnO nanofibers was investigated by successively increasing of the contact time from 5 to 350 min (Fig. 7). The quantity of Pb^{2+} adsorbed onto the PAN/ZnO nanofibers was found to increase steadily with time and equilibrium was attained at about 30 min. After equilibrium, the adsorption rate was observed to remain nearly constant. The apparently high rate of adsorption in the first 30 min could be attributed to the fact that the available adsorption sites were sufficient when compared with the density of Pb^{2+} adsorbed at the beginning. With further increase in time, the adsorption sites become saturated gradually. Finally, all possible adsorption sites will be occupied and from then on, a dynamic equilibrium in which Pb^{2+} ions adsorbed onto the PAN/ZnO nanofibers surfaces are balanced by Pb^{2+} ions leaving the nanofibers surfaces. As a result, no change shall be observed in the level of Pb^{2+} adsorption.

The effect of temperature The adsorption of metal ions was carried out at different temperatures between 298 and 333 K using PAN/ZnO nanofibers as an adsorbent. The experimental results showed that the adsorption reduces with increase of solution temperature. This indicates that the adsorption of lead ions on the adsorbent is an exothermic process (Fig. 8).

The effect of adsorbent amount The amount of lead ions adsorption increased with the increase in adsorbent

**Fig. 8** Effect of temperature on adsorption of Pb^{2+} onto adsorbent [lead ions = 1.2×10^{-4} mol/l, pH 6, adsorbent (PAN + 3 % ZnO nanocomposite) weight = 0.03 g, equilibration time = 30 min]**Fig. 9** The effect of adsorbent amount on adsorption of Pb^{2+} onto adsorbent (lead ions = 1.2×10^{-4} mol/l, pH 6, equilibration time = 30 min, 298 K)

dosage and reached a maximum value after a particular dose (Fig. 9). The optimum metal ions removal was observed at 0.03 g of PAN/ZnO nanofibers. The increase in the adsorption of metal ions with nanofibers dosage was due to the introduction of more binding sites for adsorption and the availability of more surface area.

Effect of pH The pH of the solution has been reported as an important factor in adsorption processes. The pH of the system controls the adsorption capacity due to its influence on the surface properties of the adsorbent. Adsorption experiments were carried out in the pH range of 1.5–6, keeping all other parameters constant, (contact time = 30 min, adsorbent dose = 0.03 g, and room temperature) while initial lead ion concentration was 1.2×10^{-4} mol/l. As depicted in Fig. 10, the maximum removal of lead ions was at pH 6. There was a sharp increase in adsorption with an increase in pH of the aqueous solution due to the fact that at low pH, because of high-proton concentration, positive charge density on the adsorbent increases and lead ions are fended off. pH increasing causes higher

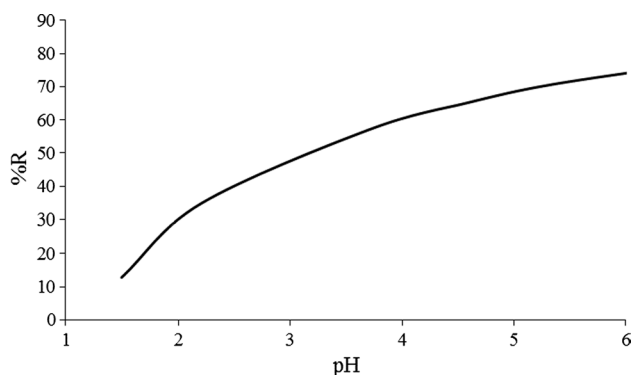


Fig. 10 Effect of pH on adsorption of Pb²⁺ onto adsorbent (lead ions = 1.2×10^{-4} mol/l, adsorbent [PAN + 3 % ZnO nanocomposite) weight = 0.03 g, equilibration time = 30 min, 298 K]

negative charge density on the adsorbent so cation adsorption enhances due to deprotonation of cations. Probably partial hydrolysis of metal ions causes a consequent reduction in adsorption capacity. Above pH 6, lead ions precipitated and experiments were not done at higher pH values.

By considering this result, and the two outcomes of the last section, optimum operational condition was figured to be: temperature 298 K, contact time 30 min, and pH 6. Under the optimized conditions, the distribution coefficient of the lead ions on this adsorbent ($K_d = 11,208.33$ ml/g) shows good affinity of this material for Pb(II) cations in water.

Adsorbent regeneration In this section, we have investigated whether the adsorbent still has an adsorption effect after the adsorption and how many times the adsorbent keeps its regeneration. For this purpose, 0.03 g of the adsorbent was placed in the shaker in contact with 30 ml of 1.2×10^{-4} mol/l Pb(II) for 30 min. After this time, the adsorbent was removed from the solution and placed in contact with distilled water for 24 h to remove Pb ions. After drying the adsorbent at 333 K, it was subjected to a second run of the batch adsorption process with the same concentration of metal ions. This procedure was repeated three times. After each adsorption step, the concentrations of solution were measured through ICP analysis and they are presented in Table 2 for comparison.

As can be observed, the adsorbent can be regenerated by suitable desorption processes for multiple uses without significant loss of its adsorption capacity.

Adsorption isotherm Equilibrium data, commonly known as adsorption isotherms, are basic requirements for the design of adsorption system. The equation parameters and the underlying thermodynamic assumptions of these equilibrium models often provide some insight into both the adsorption mechanism and the surface properties and affinity of the adsorbent. In this study, the Langmuir, Freundlich, and Temkin isotherm models were used to fit the

Table 2 Removal efficiency (*R*%) of lead ions after regeneration of adsorbent

Regeneration cycle	<i>R</i> (%)
1	71.25
2	63.64
3	60.19
4	57.72

Lead ions = 1.2×10^{-4} mol/l, adsorbent (PAN + 3 % ZnO nanocomposite) weight = 0.03 g, equilibration time = 30 min, pH 6, 298 K

experimental data and analyzed at the optimized temperature (298 K).

Langmuir adsorption isotherm models the monolayer coverage of the adsorption surfaces and assumes that adsorption occurs on a structurally homogeneous adsorbent, and all the adsorption sites are energetically identical. The linearized form of the Langmuir equation is given by Eq. (4), [25]:

$$\frac{C_e}{q_e} = \frac{1}{Q^0 b} + \frac{1}{Q^0} C_e, \quad (4)$$

where q_e (mg/g) is the adsorbate amount adsorbed by 1 g of the adsorbent, C_e (mg/l) is the equilibrium concentration of the adsorbate in the solution, Q^0 is the monolayer adsorption capacity (mg/g), and b is the constant related to the adsorption intensity.

The Freundlich isotherm model is valid for multilayer adsorption process with a nonuniform distribution of heat of adsorption on heterogeneous surfaces [29]. This empirical equation and the linear forms are given as Eqs. (5) and (6), [29]:

$$q_e = K_F C_e^n, \quad (5)$$

$$\log q_e = \log K_F + n \log C_e, \quad (6)$$

where K_F [$\text{mg g}^{-1} \times (1 \text{ mg}^{-1})^n$] is Freundlich constant related to the adsorption capacity. The parameter n is Freundlich constant representing the degree of dependence of the adsorption on the equilibrium concentration.

The derivation of the Temkin isotherm assumes that due to adsorbate/adsorbent interaction, the heat of adsorption decrease linearly rather than logarithmically, as implied in the Freundlich equation. The Temkin isotherm is given in the following equations Eqs. (7, 8), [30]:

$$q_e = \frac{RT}{b} \ln(K_T C_e), \quad (7)$$

$$q_e = A + B \ln C_e, \quad (8)$$

where $A = (RT/b) \ln K_T$ and $B = RT/b$, R is the universal gas constant (8.314 J/mol K), T is the temperature (K), K_T is equilibrium binding constant (l/g), and b is related to heat of adsorption (J/mol). Therefore, a plot of q_e versus $\ln C_e$ enables one to determine the constants.

The estimated parameters of the isotherm models are reported in Table 3. Higher correlation coefficient showed that Langmuir model described the experimental data better than Freundlich and Temkin models, which may be due to the homogeneous distribution of active sites on the nano adsorbent.

The plot of C_e/q_e versus C_e for the adsorption of Pb^{2+} on the PAN/ZnO nanofibers is shown in Fig. 11.

Thermodynamic parameters In order to evaluate thermodynamic parameters of Pb(II) ions adsorption on PAN/ZnO fibers, the plot of $\ln(K_d)$ as a function of $1/T$ was detected (Fig. 12).

From the slope and intercept of the plot and using the following equation ΔH^0 and ΔS^0 can be evaluated (Eq. 9), [27]:

Table 3 Isothermal adsorption models for the adsorption of lead (II) by PAN/ZnO nanofibers

Langmuir isotherm		
Q^0 (mg/g)	B (l/mg)	R^2
185.185	0.0096	0.9649
Freundlich isotherm		
K_f (mg ¹⁻ⁿ l ⁿ g ⁻¹)	n	
4.102	0.4707	0.93331
Temkin isotherm		
b (J/mol)	K_T (l/g)	
72.00	0.157	0.9264

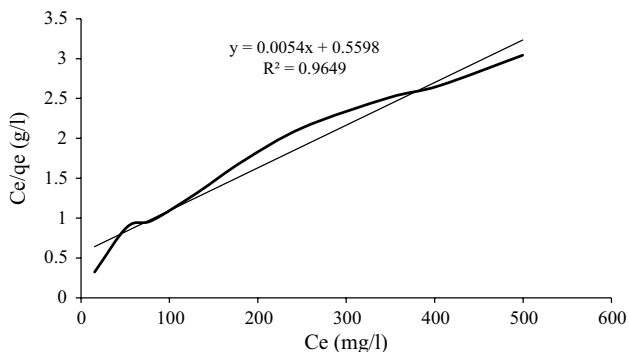


Fig. 11 Langmuir plot for the adsorption of lead (II) ions onto adsorbent [adsorbent (PAN + 3 % ZnO nanocomposite) weight = 0.03 g, pH 6, equilibration time = 30 min, 298 K]

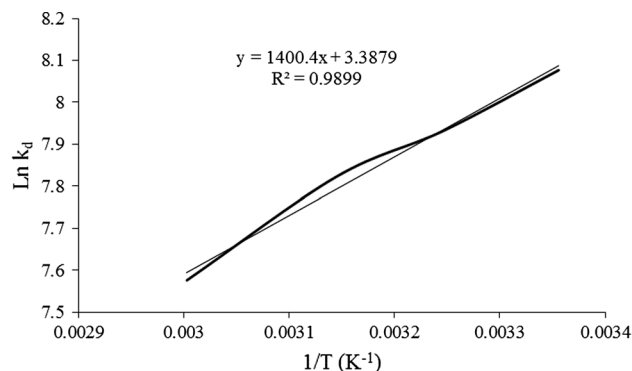


Fig. 12 Van't Hoff plot for adsorption of lead (II) ions onto adsorbent [adsorbent (PAN + 3 % ZnO nanocomposite) weight = 0.03 g, pH 6, equilibration time = 30 min]

Table 4 Thermodynamic parameters for the adsorption of lead (II) ions by PAN/ZnO nanofibers

T (K)	ΔG^0 (KJ/mol K)
298	-19.984
308	-20.264
318	-20.544
333	-20.964

$$\ln(K_d) = \frac{\Delta S^0}{R} - \frac{\Delta H^0}{RT} \tag{9}$$

free energy of adsorption can be calculated by following equation:

$$\Delta G^0 = \Delta H^0 - T\Delta S^0 \tag{10}$$

The thermodynamic results are incorporated in Table 4. The negative value of overall free energy changes indicates that the process is spontaneous and the negative value of the enthalpy change corresponds to an exothermic adsorption of lead (II) on PAN/ZnO fibers. The positive value of entropy change illustrates the increased randomness at the solid/solution interface and maybe it reflects considerable changes occur in the structure of the adsorbent during the adsorption process.

Adsorption kinetics Several models can be used to express the mechanism of solute adsorption onto an adsorbent.

In order to investigate the adsorption kinetics, four kinetic models including pseudo-first-order, pseudo-second-order, intra-particle diffusion, and Elovich models were applied to the experimental data. According to the pseudo-first-order kinetic model, the adsorption rate is proportional

to the number of free sites. The rate constant of adsorption can be determined using Eq. (11), [31]:

$$\log(q_e - q_t) = -\frac{k_1 t}{2.303} + \log q_e, \quad (11)$$

where q_e and q_t (mg/g) are the adsorption capacities at equilibrium and at any time, respectively. k_1 (min^{-1}) is the pseudo-first-order rate constant for adsorption and can be obtained from Eq. (11).

According to the pseudo-second kinetic model, the rate-limiting step is the surface adsorption that involves chemisorption, where the removal from a solution is due to physicochemical interactions between the two phases [32]. The model is usually represented by its linear form as shown in Eq. (12), [26].

$$\frac{t}{q_t} = \frac{1}{K_2 q_e^2} + \frac{t}{q_e}, \quad (12)$$

where k_2 is the second-order constant in terms of $\text{g}/(\text{mg} \cdot \text{min})$, q_e and q_t are lead uptakes (mg/g) at equilibrium and at any time during the experiment.

According to the intra-particle diffusion kinetic model, diffusion phenomenon is the rate-controlling step [33, 34] and can be described by the Eq. (13):

$$q_t = k_{id} t^{0.5} + C, \quad (13)$$

where k_{id} ($\text{mg g}^{-1} \text{min}^{-0.5}$) is the intra-particle diffusion rate constant and C (mg g^{-1}) is the boundary layer thickness. The value of C is proportional to the boundary layer effect on the adsorption process and can be calculated from Eq. (13) by plotting q_t against $t^{0.5}$, if a single-straight line passing through the origin ($C=0$) is produced, then intra-particle diffusion only controls the adsorption process. If multi-linear portions are yielded, then two or more mechanisms like external diffusion, pore diffusion, surface diffusion, and adsorption onto the pore surface influence the adsorption process.

Elovich equation is written as Eq. (14), [30]:

$$\frac{dq_t}{dt} = \alpha \exp(-\beta q_t), \quad (14)$$

$$q_t = \frac{1}{\beta} \ln(\alpha\beta) + \frac{1}{\beta} \ln(t), \quad (15)$$

where α and β are the initial adsorption rate (mg/g min) and the desorption constant (g/mg). The kinetic parameters of the described models were calculated for lead adsorption (Table 5).

These results explain that the pseudo-second-order sorption mechanism is predominant and that the overall rate constant of each sorption process appears to be controlled by the physicochemical process (Fig. 13).

Table 5 Kinetic parameters for the adsorption of lead (II) ions by PAN/ZnO nanofibers

Pseudo-first-order	
k_1 (min^{-1})	0.0097
q_e (mg/g)	3.8761
R^2	0.61
Pseudo-second-order	
k_2 ($\text{g}/\text{mg min}$)	0.026367
q_e (mg/g)	12.285
R^2	0.99
Intra-particle diffusion	
k_{id} ($\text{mg}/\text{g min}^{0.5}$)	1.5494
C (mg/g)	9.3306
R^2	0.70
Elovich equation	
α ($\text{mg}/\text{g min}$)	2.91116
β (g/mg)	0.673945
R^2	0.86

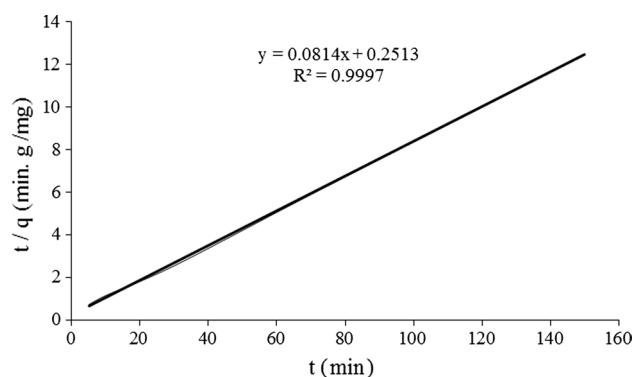


Fig. 13 Pseudo-second-order kinetic plot for the adsorption of lead (II) ions on PAN/ZnO nanofibers [adsorbent (PAN + 3 % ZnO nanocomposite) weight = 0.03 g, pH 6, 298 K]

The coefficient of correlation for the pseudo-second-order kinetic model (0.99) was higher than the pseudo-first-order (0.61), intra-particle diffusion kinetic (0.70) and Elovich (0.86) models. Accordingly pseudo-second-order kinetic model successfully described the kinetics of lead ions adsorption suggesting that the rate-limiting step was physicochemical adsorption rather than diffusion.

Conclusion

The removal of lead ions from aqueous solution was carried out in a batch adsorption mode using PAN/ZnO nanofibers adsorbent. ZnO/PAN nanofibers were prepared by electrospinning method. This adsorbent exhibited effectiveness

in the removal of Pb(II) ions from aqueous solutions. The removal efficiency was controlled by solution pH, adsorbent concentration, and contact times.

As a result of investigation of effective parameters, the optimum conditions achieve at pH 6 and time 30 min. The adsorption enhances with increasing adsorbent amount. The thermodynamic parameters indicate spontaneous ($\Delta G^0 < 0$) and endothermic ($\Delta H^0 < 0$) process. The equilibrium data fit very well with the Langmuir isotherm equation. The second-order kinetic equation best described the sorption kinetics.

Acknowledgments The author is thankful from Nuclear Science and Technology Research Institute for the financial support of this project.

References

1. K. Srinivasa Rao, D. Sarangi, P.K. Dash, G. Roy Chaudhury, *J Chem Technol Biotechnol* **77**, 1107 (2002)
2. A. Gundogdu, D. Ozdes, C. Duran, V. Numan Bulut, M. Soylak, H. Basri Senturk, *Chem Eng J* **153**, 62 (2009)
3. M. Soylak, S. Yigit, *At Spectrosc* **36**, 49 (2015)
4. B. Gao, Y. Gao, Y. Li, *Chem Eng J* **158**, 542 (2010)
5. A.W. Mohammad, R. Othaman, N. Hilal, *Desalination* **168**, 241 (2004)
6. V.V. Panchanadikar, R.P. Das, *Int J Environ Stud* **46**, 243 (1994)
7. C.J. Buchko, L.C. Chen, Y. Shen, D.C. Martin, *Polymer* **40**, 7397 (1999)
8. Y. Sang, F. Li, Q. Gu, C. Liang, J. Chen, *Desalination* **223**, 349 (2008)
9. Y. Sang, Q. Gu, T. Sun, F. Li, C. Liang, *J Hazard Mater* **153**, 860 (2008)
10. P. Gibson, H. Schreuder-Gibson, D. Rivin, *Colloid Surf* **187**, 469 (2001)
11. G. Moroi, D. Bilba, N. Bilba, *Polym Degrad Stabil* **84**, 207 (2004)
12. S. Deng, R. Bai, J.P. Chen, *J Colloid Interface Sci* **260**, 265 (2003)
13. Y.C. Sharma, V. Srivastava, V.K. Singh, S.N. Kaul, C.H. Weng, *Environ Technol* **30**, 583 (2009)
14. T. Madrakian, A. Afkhami, N. Rezvani-jalal, M. Ahmadi, *J Iran Chem Soc* **11**, 489 (2014)
15. M. Emadi, E. Shams, *J Iran Chem Soc* **10**, 325 (2012)
16. S. Bakhshayesh, H. Dehghani, *J Iran Chem Soc* **11**, 769 (2014)
17. S.G. Wang, W.X. Gong, X.W. Liu, Y.W. Yao, B.Y. Gao, Q.Y. Yue, *Sep Purif Technol* **58**, 17 (2007)
18. H. Wang, X. Lu, Y. Zhao, C. Wang, *Mater Lett* **60**, 2480 (2006)
19. D.H. Yu, R.X. Cai, Z.H. Liu, *Spectrochim Acta Part A* **60**, 1617 (2004)
20. M.L. Curridal, R. Comparelli, P.D. Cozzli, G. Mascolo, A. Agostiano, *Mater Sci Eng C* **23**, 285 (2003)
21. H.M. Lin, S.J. Tzeng, P.J. Hsiau, W.L. Tsai, *Nanostruct Mater* **10**, 465 (1998)
22. A.K. Li, W.T. Wu, *Key Eng Mater* **247**, 405 (2003)
23. R.Y. Hong, J.H. Li, L.L. Chen, D.Q. Liu, H.Z. Li, Y. Zheng, J. Ding, *Powder Technol* **189**, 426 (2009)
24. D. Litmanovich, N.A. Plate, *Macromol Chem Phys* **201**, 2176 (2000)
25. S.J. Ahmadi, S. Sadjadi, M. Hosseinpour, *Sep Sci Technol* **47**, 1063 (2012)
26. S. Mehdizadeh, S. Sadjadi, S.J. Ahmadi, M. Outokesh, *IJEHSE* **12**, 1 (2014)
27. M. Shojaei, S. Sadjadi, M. Rajabi-Hamane, S.J. Ahmadi, *Desalin Water Treat* **56**, 1403 (2015)
28. K. Saeed, S. Haider, T. Oh, S. Park, *J Membr Sci* **322**, 400 (2008)
29. G.D. Vuković, A.D. Marinković, M. Čolić, M.Đ. Ristić, R. Aleksić, A.A. Perić-Grujić, P.S. Uskoković, *Chem Eng J* **157**, 238 (2010)
30. S. Kasap, H. Tel, S. Piskin, *J Radioanal Nucl Chem* **289**, 489 (2011)
31. S. Lagergren, *Handler* **24**, 1 (1898)
32. D. Robati, *J Nanostruct Chem* **3**, 1 (2013)
33. N. Chiron, R. Guilet, E. Deydier, *Water Res* **37**, 3079 (2003)
34. E. Da'na, N. De Silva, A. Sayari, *Chem Eng J* **166**, 454 (2011)